# Resorption of, and bone formation from, new β-tricalcium phosphate-monocalcium phosphate cements: An *in vivo* study

**Kouichiro Ohura,[1] Marc Bohner,[2] Pierre Hardouin,[1,*] Jacques Lemaître,[2] Gilles Pasquier,[1] and Brigitte Flautre[1]**

*[1]IRMS, Institut Calot, Rue du Docteur Calot, 62608 Berck sur Mer Cedex, France; [2]Laboratory of Powder Technology, Materials Department, EPFL, MX-D, CH-1015 Lausanne, Switzerland*

Hard cylinders (4.7 × 10 mm) of two kinds of β-tricalcium phosphate-monocalcium phosphate monohydrate-calcium sulfate hemihydrate (β-TCP-MCPM-CSH) cements with and without β-TCP granules (500–1000 μm) were implanted into holes drilled in rabbit femoral condyles for up to 16 weeks. Empty cavities were used as control. Cement resorption and new bone formation in the cylinders were evaluated with contact microradiography and quantified through an automatic image analysis system. At 4 weeks, both kinds of cement cylinders were surrounded by new bone. At 8 weeks, except for β-TCP granules, both cement cylinders were almost completely resorbed and replaced by bone tissue. At 16 weeks the bone in the cavities of both cements recovered a trabecular pattern, but only the bone trabeculae in the initial cavity of the cement with β-TCP granules became thick and mature. However, the cavities of the empty control were still empty and large. These results show that the β-TCP-MCPM-CSH cements stimulate bone formation and are rapidly replaced by bone tissue. When added with nonresorbable β-TCP granules, this cement maintains bone formation for a longer time. 

## INTRODUCTION

Calcium phosphate cement (CPC) forms a plastic paste upon mixing with water and hardens with time.[1–3] The plasticity of the cement pastes makes them easy to fit the shape of bone defects and their subsequent hardening *in situ* ensures functional loading of the region. Furthermore, the CPCs that consist essentially of calcium phosphate compounds are highly biocompatible.

A newly developed CPC consists of mixtures of β-tricalcium phosphate (β-TCP) and monocalcium phosphate monohydrate (MCPM), to which some calcium sulfate hemihydrate (CSH) is added.[4] The setting reaction is

$$Ca(H_2PO_4)_2 \cdot H_2O + Ca_3(PO_4)_2 + 7H_2O \rightarrow 4CaHPO_4 \cdot 2H_2O$$

where the product is dicalcium phosphate dihydrate (DCPD). The heat of reaction is very low, amounting to about 5% of the heat of polymerization of polymethyl methacrylate (PMMA).[5] The reaction results in a large increase of the solid volume fraction, leading to a significant decrease of the total cement porosity (38 vol %). Hardening occurs as a result of the remaining β-TCP grains being bound together by the precipitated DCPD crystals. CSH works as a setting retardant and contributes to increasing the strength of the hardened cement by promoting the development of a fine grained microstructure. Setting time and hardening time are about 10 min and 2 h, respectively, and compressive strength is about 25–35 MPa (J. Lemaître, personal communication).

Due to their chemical composition and porous structure, β-TCP-MCPM-CSH cements are resorbable and osteoconductive.[1,4,6–9] The ideal bone substitute is a material that will be replaced by new bone.[10,11] It is possible to develop a bioresorbable bone cement with the β-TCP-MCPM-CSH cements that will allow the normal bone healing and remodeling procedure to occur.

The purpose of this study is to investigate the resorption and bone formation of two kinds of β-TCP-MCPM-CSH cements. Because the filling of implanted sites with injected plastic cement is difficult to estimate quantitatively, it was decided to implant

*To whom correspondence should be addressed.

Journal of Biomedical Materials Research, Vol. 30, 193–200 (1996)

CCC 0021-9304/96/020193-08

**TABLE I**
**Chemical Composition of β-TCP-MCPM-CSH Cements (Wt %)**

| Composition | Cement A | Cement B |
|---|---|---|
| β-Tricalcium phosphate | | |
| <250 μm | 41.7 | 34.9 |
| 500–1000 μm | | 16.3 |
| Monocalcium phosphate monohydrate | 13.0 | 10.9 |
| Calcium sulfate hemihydrate | 10.4 | 8.7 |
| Distilled water | 34.9 | 29.2 |

the cements in the form of prehardened cylinders with a well-defined geometry.

## MATERIALS AND METHODS

### Materials

The compositions of β-TCP-MCPM-CSH cements are shown in Table I. β-TCP powder (<250 μm) was prepared by calcining the mixture of hydroxyapatite (HA) and DCPD powders (molar ratio Ca/P = 1.45) at 1250°C for 4 h in nitrogen atmosphere. The resulting β-TCP was ground until all the powder passed through a standard wire cloth sieve of 250 μm. The phase purity check of the powder by X-ray diffraction demonstrated that its α-TCP content was below 10 wt %. β-TCP granules (500–1000 μm) were prepared as follows. Calcium-deficient HA (Merck, Ca/P = 1.50) was suspended in demineralized water. The suspension was filtered and the filtration cake was dried in an oven at 110°C. The dry cake was then crushed and the 500–1000 μm fraction was selected by sieving. The obtained granules were calcined two times in air at 1150°C for 16 h. These granules were multiporous and their relative density was 95%. All other ingredients were commercially available reagent grade chemicals. These powder and granules were sterilized by 25 kGy γ irradiation.

At the time of implantation, 2.5 g of cement A and 3.25 g of cement B were mixed with 1.34 g of distilled water for 60 s and injected into the cylindrical polypropylene mold to make preformed specimens with a diameter of 4.7 mm and length of 10 mm.

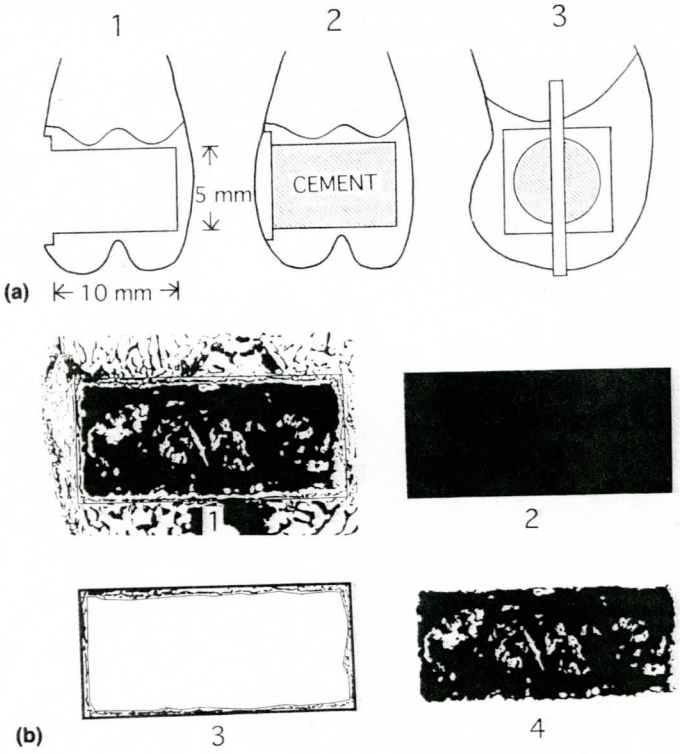


**Figure 1.** (a) Schematic drawing of (1) the drilled cavity, (2) the implanted cement cylinder, and (3) the section plane of the histological preparations. (b) Schematic drawing of the morphometrical measurement using automatic image analysis system (Fig. 2, Cement A): (1) Digitized image through a black and white video tube camera. The outline of new bone frame was traced. (2) After erasing the image outside of this trace, the area inside was homogenized. (3) The periphery of new bone was traced. After erasing the image inside of this trace, the area of new bone was pseudocolored using thresholds. (4) After erasing the image outside, the area of free cement was pseudocolored.

### Surgical procedure

Using sterile surgical technique and general anesthesia, the distal femoral condyle of 28 adult female New Zealand white rabbits, weighing between 3.5 and 5.0 kg, was exposed through lateral incision and an 8 × 8 mm cortical bone plug was excised [Fig.

**TABLE II**
**Area of Empty Cavities and Free Cement Residues Surrounded by New Bone**

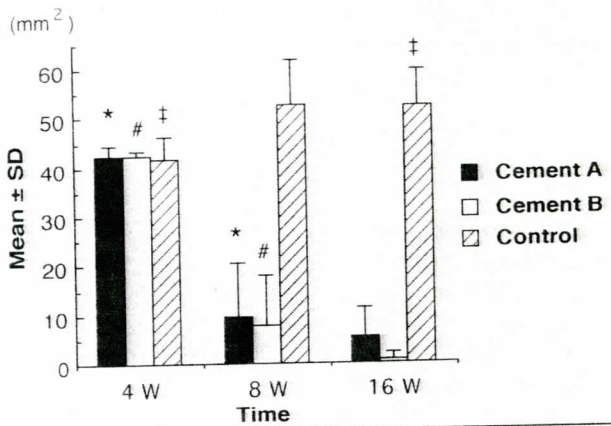


Values were significantly different in pairs. Mann-Whitney $U$ test, two-way analysis, $p < 0.05$.

TABLE III
Area of Unresorbed Free Cement Including Free β-TCP Granules and Area of β-TCP Granules

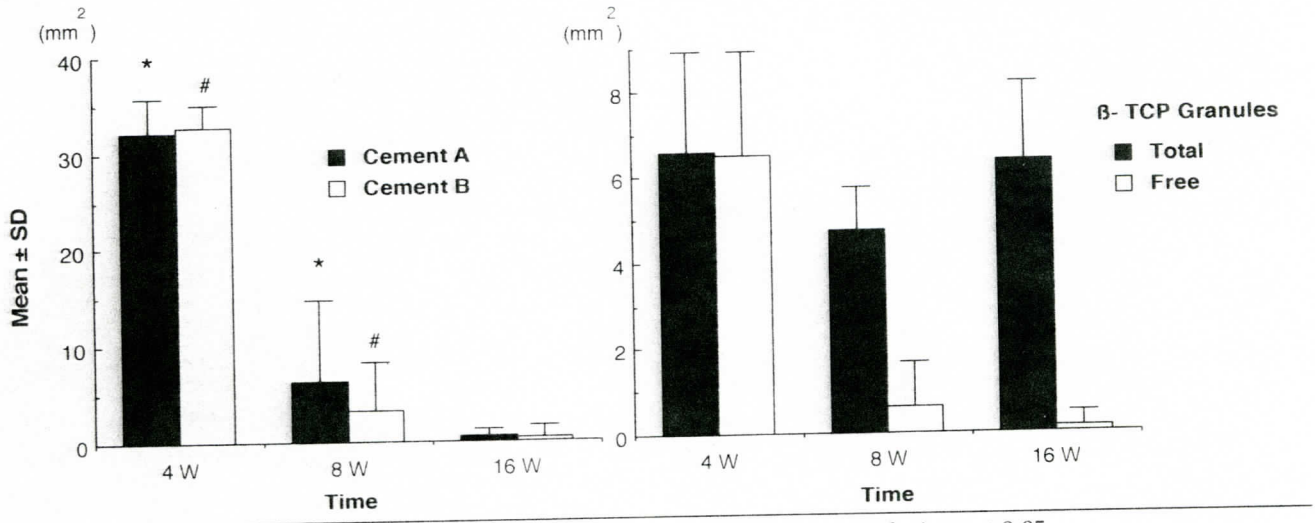


Values were significantly different in pairs. Mann–Whitney $U$ test, two-way analysis, $p < 0.05$.

1(a)].[12] Through this bone defect, a 5-mm cylindrical cavity was made into the cancellous bone with drills and carefully rinsed with saline.

The procedure was performed on both sides. The cavities were filled with two kinds of cement cylinders or left empty according to the randomization. The bone plug was replaced in its original place without support. Animals were sacrificed at 4, 8, and 16 weeks. Thus, results of six specimens in each group at each stage, except eight specimens in the cement B group at 16 weeks, were available. IRMS guidelines for the care and use of laboratory animals were observed.

TABLE IV
Area of New Bone within Initial Cement Cylinder Including Cement Residues Incorporated into Bone

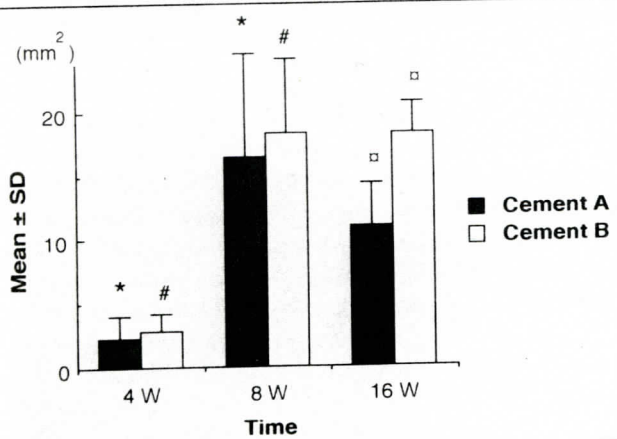


Values were significantly different in pairs. Mann–Whitney $U$ test, two-way analysis, $p < 0.05$.

## Radiographic analysis and histology

After sacrifice, the femoral condyles were excised and fixed in 10% phosphate-buffered formaldehyde solution. These specimens were then dehydrated in ethanols and embedded in PMMA. Each specimen was sawn every 500 μm (Isomet saw, Buehler, Ltd.) parallel to the implant axis [Fig. 1(a)]. The slices were hand polished to 100 μm and microradiographed. The 100-μm slices were further polished to around 10 μm by a Micro Grinding System (Exakt, Germany) and stained with Giemsa solution for histomorphometry. After sawing the center slice of the cement cylinder, the residual PMMA block was prepared for scanning electron microscopy (S360, Cambridge, U.K.).

The quantitative evaluation of cement resorption and bone formation was made from the microradiographs using an automatic image analysis system (Vidas, Kontron, Germany).[14] The microradiograph was digitized through a black and white video tube camera and the outline of a new bone frame was traced [Fig. 1(b-1)]. After erasing the image outside of this trace, the area inside was homogenized and computed [Fig. 1(b-2)]. Then the slice with the maximal cross section of each cement cylinder was selected.

Using this slice, the values in Tables II–IV were measured. The periphery of new bone including the cement residues incorporated into the bone was traced [Fig. 1(b-3)]. The area inside of this trace, the area of empty cavities and free cement residues surrounded by new bone, was computed using the tech-

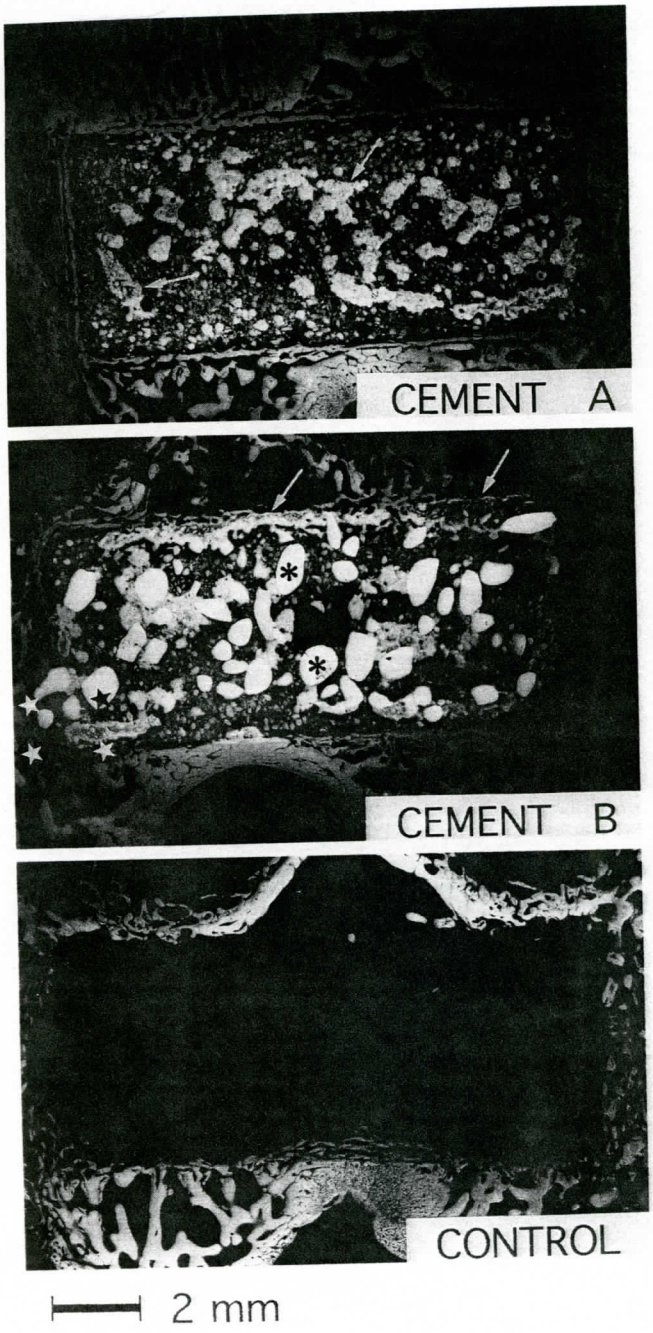


**Figure 2.** Contact microradiographs 4 weeks after implantation: (★★★★) area of Figure 4(a); (✱) β-TCP granule; and (←) condensed cement.

nique mentioned above. To distinguish the two zones of similar mineral contents, areas of indifference were erased before measurement. The areas of interest were pseudocolored and computed using thresholds: unresorbed free cement including free β-TCP granules [Fig. 1(b-3)], and new bone within the initial cement cylinder including the cement residues incorporated into the bone [Fig. 1(b-4)]. The area of β-TCP granules was independently measured.

## RESULTS

### Radiographic analysis and histology

At 4 weeks, both kinds of cement cylinders were surrounded by newly formed bone tissue (Fig. 2). Except for β-TCP granules and the high density condensed cement areas scattered in the cylinders, all cement cylinders became low density owing to the dissolution of smaller cement particles. At the surface of the cylinders, except the condensed cement areas, all the cement components were resorbed and both cement cylinders were reduced in diameter. New bone could not reach to the cylinder surface of these resorbed areas but reached to those of β-TCP granules and the condensed cement areas. In the surroundings of the empty control cavity, low amounts of new bone and an incomplete bone frame were formed.

In cement B some β-TCP granules near the surface of the cylinders were incorporated into the bone tissue (Fig. 2). These microporous β-TCP granules filled their micropores with new bone (Fig. 3).

The newly formed bone trabeculae displayed a layer of active osteoblasts directly attached to the β-TCP granules and the condensed cement areas [Fig. 4(a)]. Some chronic inflammation involving histiocytes was observed in the space among cement remnants. Foreign body giant cells were occasionally present around the cements [Fig. 4(b)].

At 8 weeks, except for β-TCP granules, both cements were almost completely resorbed and replaced by bone tissue (Fig. 5). The spaces in which both cements had been implanted were occupied with the high density mixture of bone and cement residues. New bone did not develop in the control cavity.

The high density area consisted of bone tissue incorporating cement residues (Fig. 6). β-TCP small granules were the main constituent of the cement residues. Other cement particles had already disappeared.

At 16 weeks, as the cement residues disappeared, bone remodeling occurred (Fig. 7). The bone trabeculae within the initial cement A cylinder were still thin and immature, but those within the cement B cylinder, which formed a network with the bone outside of the cylinder, became thick and mature. The control cavity was nearly the same as that at 8 weeks.

In cement B β-TCP granules were incorporated into bone tissue and became a part of the bone trabeculae (Fig. 8). The bone marrow structure was recovered among the bone trabeculae.

### Quantitative data

The area surrounded by new bone was the same at 4 weeks among the three groups (Table II). This area

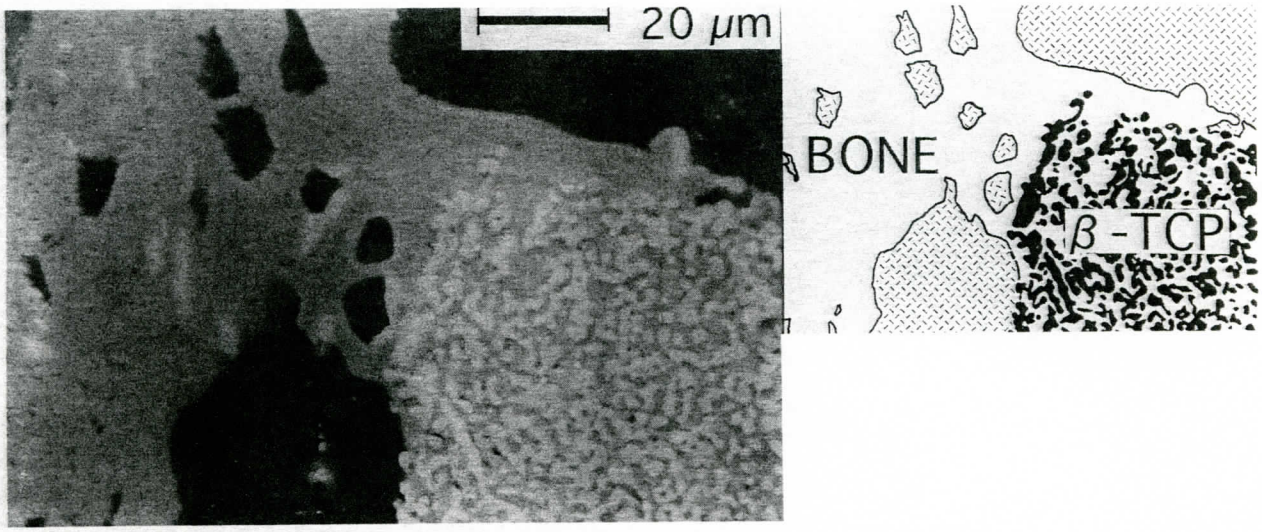


**Figure 3.** Interface scanning electron microscopy of cement B cylinder 4 weeks after implantation. From left side, new bone incorporated a microporous β-TCP granule at the surface of the cylinder and filled its cavity completely: (□) bone and (■) β-TCP.

decreased very much in both cement groups at 8 weeks, but that of the control group became larger at 16 weeks.

The initial value of the cement area measured using cement cylinders was 39.47 ± 1.87 ($n$ = 4) in cement A and 39.18 ± 1.41 ($n$ = 3) in cement B. The unresorbed free cement area decreased about 15% in both cement groups at 4 weeks (Table III). This area became very small in both groups and the β-TCP granules were almost incorporated into the bone tissue at 8 weeks.

New bone formation within the initial cement cylinder was still low in both cement groups at 4 weeks (Table IV). After the resorption of the cements, this value increased about seven times in both groups at 8 weeks and was maintained in cement B group. However, in cement A group the formed bond decreased again at 16 weeks.

## DISCUSSION

A cancellous bone defect model in rabbits was used. Because the bone defect could not be filled spontaneously with regenerated bone in this test model with a size of 5 mm, it is possible to compare the resorption and new bone formation of different materials in the same conditions.[12]

The automatic image analysis system is an efficient means to quantify implant resorption and bone formation.[13,14] However, it is difficult to distinguish the cement remnant and the microporous β-TCP granules incorporated into bone tissue from pure bone. In this study, the cement remnant in the bone was small and the micropores of β-TCP granules were occupied by bone tissue. Therefore, we dealt with them as bone tissue. Furthermore, it is difficult to measure precisely the heterogeneous cement with small grains with this system. The reason why the initial amounts of the cements showed low values is caused by ignorance of the low density area at the measurement. It is better to realize that the true value of the cement remnant is between the area of empty cavity and the area of free cement.

Results revealed that both kinds of β-TCP-MCPM-CSH cements, except β-TCP granules, were almost completely resorbed and replaced by new bone in 8 weeks. Therefore, the size of cavities of these groups became very small, when compared to the control empty cavity. However, there was no difference in the cavity size at 4 weeks between the cement groups and the control cavity. This suggested that the osteoconductive β-TCP-MCPM-CSH cement had obviously stimulated bone formation but had not accelerated the rate of bone formation.

After disappearance of the cement, remodeling of the formed bone occurred in both cement groups at 16 weeks. The bone volume in the cavity of the cement with β-TCP granules was maintained, but that of the cement without β-TCP granules was not. This suggests that the nonresorbable granules maintain the stimulation of bone formation.

Munting et al. reported that the β-TCP-MCPM-CSH cement [β-TCP (500–1000 μm) 56, β-TCP (<5 μm) 8, MCPM 16, CSH 15, calcium pyrophosphate (CPP) 5 in wt %] had been resorbed slowly and showed a highly variable pattern of bone ingrowth and cement resorption.[15] They used cylinders 10 mm in diameter and 20 mm in length. Therefore, their cement needed longer time for resorption. Furthermore, they implanted the cement into both cortical

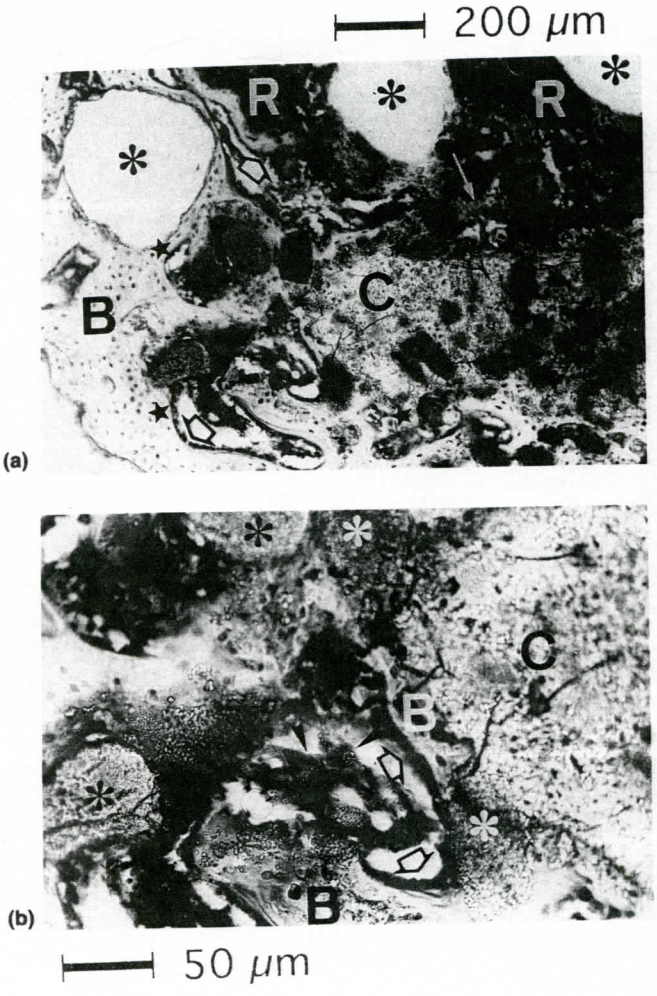


**Figure 4.** (a) Histological section of a part of cement B cylinder in Figure 2: (★★) area of Figure 4(b), (B) bone and (C) condensed cement; (✱) β-TCP granule, (R) cement residues; (◊) osteoblasts; and (←) histiocytes (Giemsa staining). (b) High magnification of Figure 4(a): (B) bone and (C) condensed cement; (✱) β-TCP granule; (◊) osteoblasts; and (➤) foreign body giant cell (Giemsa staining).

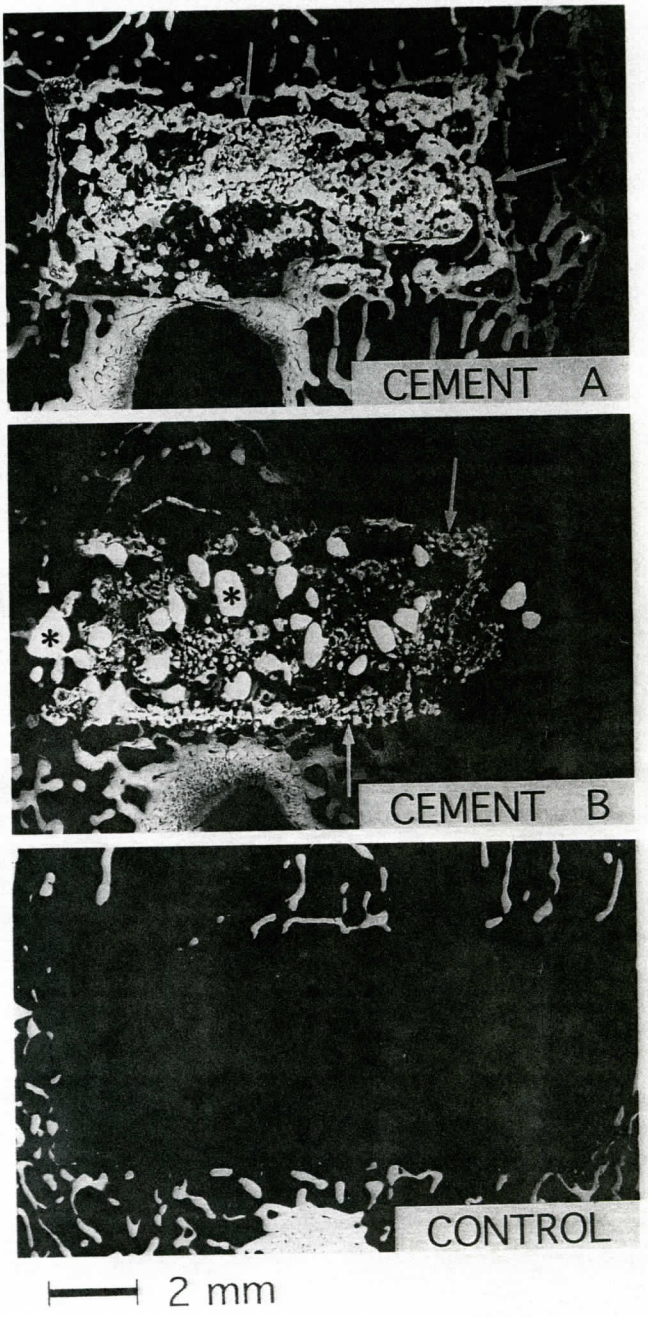


**Figure 5.** Contact microradiographs 8 weeks after implantation: (★★) area of Figure 6; (←) mixture of bone and cement residues; and (✱) β-TCP granule.

and cancellous bone so that their results showed large variation.

Various studies reported that the tetracalcium phosphate-dicalcium phosphate dihydrate (TTCP-DCPD) cement caused mild tissue irritation and was progressively replaced by bone tissue.[16–18] However, this cement was stable over 12 months with respect to shape and volume. The product of the TTCP-DCPD cement is nearly pure HA that does not have pores large enough to allow bone ingrowth by osteoconduction. Therefore, it needed a long time to be replaced by bone tissue.

Constantz et al. reported that a monocalcium phosphate monohydrate-α-tricalcium phosphate-calcium carbonate (MCPM-α-TCP-CC) paste was injectable and had the potential for replacement with natural bone.[19] Sixteen weeks after implantation, the remodeling of this paste was essentially complete in the cortical bone region, whereas little remodeling had occurred in the region of cancellous bone. The product of the MCPM-α-TCP-CC paste is dahlite (carbonated apatite), which has greater solubility than stoichiometric HA. However, the median average pore throat diameter of this product is ~300 Å. Therefore, this nanophase porous structure was supposed to be insufficient for fast bone replacement.

The β-TCP-MCPM-CSH cements after setting consisted of β-TCP, MCPM, DCPD, and calcium sulfate

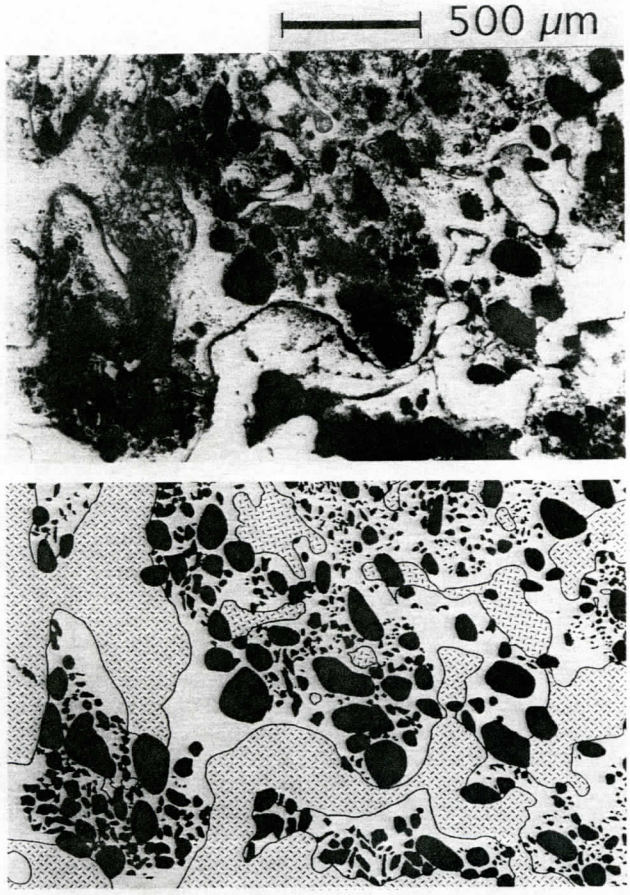


**Figure 6.** Histological section of a part of cement A cylinder in Figure 5: (□) bone and (■) β-TCP small granules and cement residues (Giemsa staining).

dihydrate (CSD).[1,4,5] The mean pore volume of the prehardened cements is 35%. The pore size distribution is in the range of 5–50 μm with a maximum around 20 μm. The porosity is essentially open and interconnected. Some spherical macropores (around 500–1000 μm) due to bubble incorporation during mixing are also present. These cements show a microstructure in which a number of small, needlelike DCPD crystals are entangled with larger β-TCP particles. After implantation, CSD dissolves first followed by the calcium phosphates according to their chemical and crystallographic nature. The composition and structure are suggested to play important roles in the fast bone replacement of β-TCP-MCPM-CSH cements.

The resorption of β-TCP-MCPM-CSH cement starts with the dissolution of its highly soluble components. The presence of foreign body giant cells shows that its small particles are phagocytized through a process of foreign body reaction. Although osteoclasts were not observed, remodeling of the formed bone and replacement of β-TCP granules by living bone are suggested to occur in a manner similar to bone remodeling.

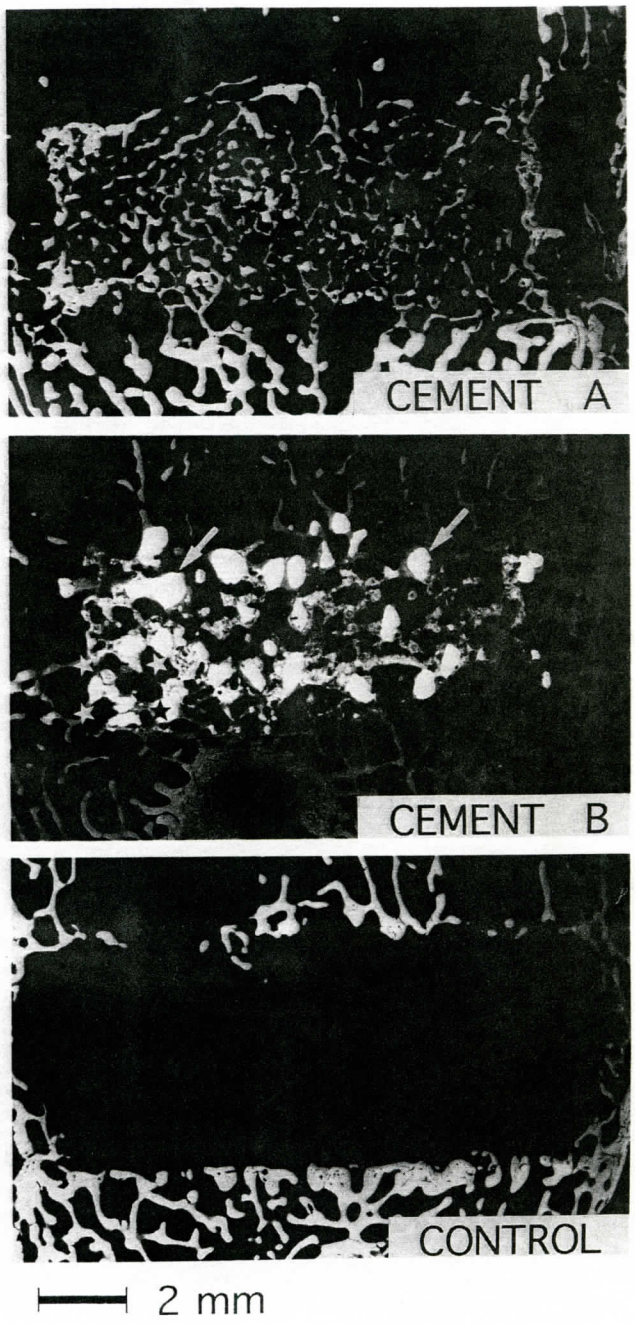


**Figure 7.** Contact microradiographs 16 weeks after implantation: (✶✶✶) area of Figure 8 and (←) β-TCP granule.

In this study, we demonstrated that the β-TCP-MCPM-CSH cements fulfill two requirements as bioresorbable cements: appropriate resorption and fast bone replacement. Some important questions about the requirements for a satisfactory bone cement were answered. However, many questions still remain unanswered, particularly about handling qualities, hardening, and mechanical properties *in vivo*.

This work was supported by a grant from the Caisse Regionale d'Assurance Maladie Nord-Picardie and Uehara Memorial Foundation. J. L. thanks the Board of the Swiss

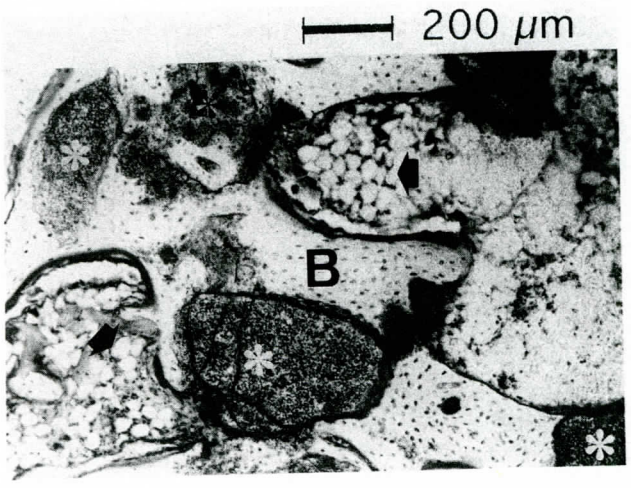


**Figure 8.** Histological section of a part of cement B cylinder in Figure 7: (✱) β-TCP granule; (B) bone; and (←) bone marrow (Giemsa staining).

Federal Institutes of Technology for financial support (Priority Program "Materials," Project 4B3).

## References

1. W. E. Brown and L. C. Chow, in *Cements Research Progress*, P. W. Brown (ed.), American Ceramics Society, Westerville, OH, 1986, pp. 352–379.
2. L. C. Chow, "Development of self-setting calcium phosphate cements," *Centen. Mem. Issue Ceramics Soc. Jpn.*, **99,** 954–964 (1991).
3. A. A. Mirtchi, J. Lemaître, and N. Terao, "Calcium phosphate cements: Study of the β-tricalcium phosphate-monocalcium phosphate system," *Biomaterials*, **10,** 475–480 (1989).
4. A. A. Mirtchi, J. Lemaître, and E. Munting, "Calcium phosphate cements action of setting regulators on the properties of β-tricalcium phosphate-monocalcium phosphate cements," *Biomaterials*, **10,** 634–638 (1989).
5. J. Lemaître, E. Munting, and A. Mirtchi, "Setting, hardening and resorption of calcium phosphate hydraulic cements," *STOMATO. 91. Proceedings, COM*, 1–5 (1991).
6. K. de Groot, "Bioceramics consisting of calcium phosphate salts," *Biomaterials*, **1,** 47–50 (1980).
7. K. Shimazaki and V. Mooney, "Comparative study of porous hydroxyapatite and tricalcium phosphate as bone substitute," *J. Orthop. Res.*, **3,** 301–310 (1985).
8. J. O. Hollinger and G. C. Battistone, "Biodegradable bone repair materials: Synthetic polymers and ceramics," *Clin. Orthop.*, **207,** 290–305 (1986).
9. P. S. Eggli, W. Muller, and R. K. Schenk, "Porous hydroxyapatite and tricalcium phosphate cylinders with two different pore size ranges implanted in the cancellous bone of rabbits," *Clin. Orthop.*, **232,** 127–138 (1988).
10. H. Ohgushi, M. Okumura, S. Tamai, E. C. Shors, and A. I. Caplan, "Marrow cell induced osteogenesis in porous hydroxyapatite and tricalcium phosphate: A comparative histomorphometric study of ectopic bone formation," *J. Biomed. Mater. Res.*, **24,** 1563–1570 (1990).
11. T. N. Gerhart, R. L. Miller, S. J. Kleshinski, and W. C. Hayes, "*In vitro* characterization and biomechanical optimization of biodegradable particulate composite bone cement," *J. Biomed. Mater. Res.*, **22,** 1071–1082 (1988).
12. B. D. Katthagen, "Bone regeneration with bone substitutes," Springer–Verlag, Berling-Heidelberg-Tokyo, 1986.
13. G. Guillemin, A. Meunier, P. Dallant, P. Christel, J. C. Pouliquen, and L. Sedel, "Comparison of coral resorption and bone apposition with two natural cords of different porosities," *J. Biomed. Mater. Res.*, **23,** 765–779 (1989).
14. P. Hardouin, D. Chopin, B. Devyver, B. Flautre, M. C. Blary, P. Guigui, and K. Anselme, "Quantitative histomorphometric evaluation of spinal arthrodesis after biphasic calcium phosphate ceramic implantation in sheep," *J. Mater. Sci. Med.*, **3,** 212–218 (1991).
15. E. Munting, A. A. Mirtchi, and J. Lemaître, "Bone repair of defects filled with phosphocalcic hydraulic cement: An *in vivo* study," *J. Mater. Sci. Mater. Med.*, **4,** 337–344 (1993).
16. Y. C. Hong, J. T. Wang, C. Y. Hong, W. E. Brown, and L. C. Chow, "The periapical tissue reactions to calcium phosphate cement in the teeth of monkeys," *J. Biomed. Mater. Res.*, **25,** 485–498 (1991).
17. C. D. Friedman, P. D. Costantino, K. Jones, L. C. Chow, H. J. Pelzer, and G. A. Sisson, "Hydroxyapatite cement: II. Obliteration and reconstruction of the cat frontal sinus," *Arch. Otolaryngol. Head Neck Surg.*, **117,** 385–389 (1991).
18. P. D. Costantino, C. D. Friedman, K. Jones, L. C. Chow, and G. A. Sisson, "Experimental hydroxyapatite cement cranioplasty," *Plast. Reconstr. Surg.*, **90,** 174–185 (1992).
19. B. R. Constantz, I. C. Ison, M. T. Fulmer, R. D. Poser, S. T. Smith, M. VanWagoner, J. Ross, S. A. Goldstein, J. B. Jupiter, and D. I. Rosenthal, "Skeletal repair by *in situ* formation of the mineral phase of bone," *Science*, **267,** 1796–1799 (1995).

Received March 31, 1994
Accepted June 19, 1995